The Astrophysical Journal, 801:3 (10pp), 2015 March 1 doi:10.1088/0004-637X/801/1/3

PHOTOMETRIC AMPLITUDE DISTRIBUTION OF STELLAR ROTATION OF KOIs—INDICATION FOR SPIN–ORBIT ALIGNMENT OF COOL STARS AND HIGH OBLIQUITY FOR HOT STARS

Tsevi Mazeh[1,2], Hagai B. Perets[3], Amy McQuillan[1], and Eyal S. Goldstein[1]
[1] School of Physics and Astronomy, Raymond and Beverly Sackler Faculty of Exact Sciences, Tel Aviv University, Tel Aviv 69978, Israel; mazeh@post.tau.ac.il
[2] The Jesus Serra Foundation Guest Program, Instituto de Astrofísica de Canarias, C. via Lactea S/N, E-38205 La Laguna, Tenerife, Spain
[3] Physics Department, Technion: Israel Institute of Technology, Haifa 32000, Israel
Received 2014 August 28; accepted 2014 December 12; published 2015 February 23

ABSTRACT

The observed amplitude of the rotational photometric modulation of a star with spots should depend on the inclination of its rotational axis relative to our line of sight. Therefore, the distribution of observed rotational amplitudes of a large sample of stars depends on the distribution of their projected axes of rotation. Thus, comparison of the stellar rotational amplitudes of the *Kepler* objects of interest (KOIs) with those of *Kepler* single stars can provide a measure to indirectly infer the properties of the spin–orbit obliquity of *Kepler* planets. We apply this technique to the large samples of 993 KOIs and 33,614 single *Kepler* stars in temperature range of 3500–6500 K. We find with high significance that the amplitudes of cool KOIs are larger, on the order of 10%, than those of the single stars. In contrast, the amplitudes of hot KOIs are systematically lower. After correcting for an observational bias, we estimate that the amplitudes of the hot KOIs are *smaller* than the single stars by about the same factor of 10%. The border line between the relatively larger and smaller amplitudes, relative to the amplitudes of the single stars, occurs at about 6000 K. Our results suggest that the cool stars have their planets aligned with their stellar rotation, while the planets around hot stars have large obliquities, consistent with the findings of Winn et al. and Albrecht et al. We show that the low obliquity of the planets around cool stars extends up to at least 50 days, a feature that is not expected in the framework of a model that assumes the low obliquity is due to planet–star tidal realignment.

Key words: methods: observational – planets and satellites: dynamical evolution and stability – planet–star interactions – stars: rotation

Supporting material: machine-readable table

1. INTRODUCTION

The photometry of the *Kepler* space mission (Borucki et al. 2010) is revolutionizing the study of stellar rotation by providing four years of almost uninterrupted light curves (LCs), with an unprecedented level of precision and time sampling, for a very large sample of stars. The data allow detection of photometric modulation induced by stellar spots that cross the stellar visible disk with the rotational period of the star. With the *Kepler* data we can detect stellar rotational periods even for slowly rotating stars with low-amplitude modulation, for a well-defined large sample (e.g., Basri et al. 2011; Nielsen et al. 2013; Reinhold et al. 2013). To derive the rotational periods from these data, McQuillan et al. (2013a, 2014) used the auto-correlation function (ACF) of each LC, which measures the degree of self-similarity of the photometry over a range of time lags. This method yielded 34,030 rotational periods for single main-sequence stars in the *Kepler* sample (McQuillan et al. 2014, hereafter MMA14). By definition, the single-star sample of MMA14 did not include any *Kepler* objects of interest (KOIs), which showed evidence for transiting planets (Batalha et al. 2013), nor detected eclipsing binaries (EB; Prša et al. 2011; Slawson et al. 2011).

Given the large sample of MMA14, we can now compare the observational statistical features of the stellar rotation of the single stars of *Kepler* with the ones of the KOIs. McQuillan et al. (2013b, hereafter MMA13) compared the stellar rotational *periods* of the KOIs with those of the single stars, while this work considers the observed photometric *amplitudes* of the two groups.

The observed rotational amplitude of a star (e.g., Basri et al. 2011; McQuillan et al. 2013a; Walkowicz & Basri 2013; MMA14) depends on the inclination of its rotational axis relative to our line of sight—stars with low rotational inclinations appear with lower observed amplitudes (e.g., Jackson & Jeffries 2012). Therefore, the distribution of the observed rotational amplitudes of a sample is not the real-amplitude distribution, as measured by an observer with a line of sight orthogonal to the stellar rotational axes. Instead, subject to an observational detection threshold, we measure the real distribution convolved with some spread function, which reflects the inclination distribution of the sample and the dependence of the amplitude on the inclination (e.g., Jackson & Jeffries 2013).

These considerations suggest that we can have some indirect access to the distribution of stellar inclinations of the *Kepler* KOIs relative to the inclinations of the single stars by comparing their observed amplitude distributions, if we assume that the distributions of their real amplitudes are the same. Naively, we could expect the stellar inclinations of the KOIs to be close to 90°, and therefore the rotational amplitudes of the KOIs to be larger than those of the *Kepler* single stars, provided the KOIs' rotational axes are aligned with the orbital inclinations of their transiting planets, which are almost orthogonal to our line of sight.

The angle between the stellar spin axis and the orbital planetary angular momentum for an individual planet, also referred to as the obliquity of the system, is a matter of intense study in recent years. It typically relies on spectroscopic measurements during transit, making use of the Rossiter–Mclaughlin (RM) effect (Queloz et al. 2000) to measure the projected obliquity on

Table 1
Stellar Rotational Periods for the KOIs

Stellar and Rotational Detection Parameters									Flags[a]
KOI	KIC	$T_{\rm eff}$ (K)	log g (g cm^{-3})	$P_{\rm rot}$ (days)	$\sigma_{\rm p}$ (days)	$R_{\rm var}$ (ppm)	LPH	w	...
3	10748390	4766	4.59	29.319	0.497	12245.86	0.61	0.43	...
42	8866102	6170	4.10	20.851	0.091	1112.76	1.02	0.52	...
49	9527334	6000	4.50	8.594	0.030	15672.53	1.23	0.68	...
82	10187017	4908	4.70	26.407	0.485	4052.73	0.72	0.49	...
85	5866724	6006	4.07	7.882	0.210	268.88	0.68	0.46	...

Notes. [a] Flags included in the full online table have the following definitions: D: values of Dressing & Charbonneau (2013) used, N: KIC values missing so NEA values used; C: centroid motion shows transit and rotational modulation on different stars; G: likely giant; T: $T_{\rm eff}$ outside the range 3500–6500 K; F: FP (EB) identified in this work; R: rejected by visual examination stage.

(This table is available in its entirety in machine-readable form.)

the sky (e.g., Triaud et al. 2010; Moutou et al. 2011; Winn et al. 2011; Albrecht et al. 2012). This was done primarily for hot Jupiters—gas-giant planets at short-period orbits. The extensive effort has lead to measurements of a few tens of spin–orbit projected inclinations.

The line-of-sight component of the spin–orbit angle can be measured using asteroseismology (Gizon & Solanki 2003; Chaplin et al. 2013), or the observed stellar rotational line broadening, *if* the host star radius and rotational period are known with sufficient precision (Hirano et al. 2012, 2014; Walkowicz & Basri 2013). Schlaufman (2010) has taken a statistical approach to identify KOIs with small stellar line broadening with respect to its expected distribution, if the stars were aligned with the planetary motion, given the stellar type and the experimental errors. He found 10 systems with probable high obliquity. Finally, at about the submission of this paper, Morton & Winn (2014) published an analysis of the observed rotational line broadening and rotational periods of 70 KOIs, obtaining posterior probability of the distribution of the stellar obliquities. They suggested with a 95% confidence level that the obliquities of stars with only a single detected transiting planet are systematically larger than those with detected multiple transiting planets.

An interesting method was applied by Nutzman et al. (2011) and Sanchis-Ojeda et al. (2011), who used brief photometric signals during transit induced by the transiting object moving across spots located on the surface of the host object. This method required identification of the "spot-crossing" event within a transit, and has been applied to additional systems using short-cadence *Kepler* LCs (e.g., Sanchis-Ojeda et al. 2013).

In a seminal work, Fabrycky & Winn (2009) noticed that some of the transiting planets were found to be aligned in a prograde orbit, with obliquity close to zero, while others were found to be misaligned, including systems in retrograde motion, where the spin–orbit angle is close to 180° (e.g., Winn et al. 2010; Hébrard et al. 2011). Fabrycky & Winn (2009) inferred the existence of two populations of hot Jupiters—well-aligned with the stellar rotational axes and isotropic. Winn et al. (2010) discovered that hot stars host high obliquity systems, while cool stars have their hot Jupiters all aligned. As also shown by Albrecht et al. (2012), the transition between the two populations occurs at effective temperature, $T_{\rm eff}$, of 6250 K. A second obliquity trend was suggested by Hébrard et al. (2011), who pointed out that retrograde planetary motion was observed only for low-mass planets, below 3 Jupiter masses (see a concise summary of the observational evidence for the obliquity distribution by Dawson 2014).

All these observational trends are crucial for our understanding the formation and dynamical evolution of planetary systems. We therefore set out to use the derived *amplitudes* of the stellar rotational photometric modulations of the KOIs and compare them to the amplitudes of the single stars observed by *Kepler*. Our goal is to confirm or refute some of the statistical trends reported, the alignment of the cool star axes with their planets in particular, and to explore the range of orbital periods for which the alignment can be traced.

Section 2 describes the target selection for the KOIs and Section 3 the derivation of the rotational periods and their amplitudes. We then compare the KOI amplitudes to those of the single-star sample of MMA14 in Section 4 and perform extensive simulations to study some possible observational biases in Section 5. Section 6 shows that a natural interpretation of our findings is that planets around cool stars have their orbits aligned with the rotational axes of their parent stars, while the hot star systems have large obliquities. Section 7 shows that the low obliquity of the cool stars extends up to at least 50 days. Section 8 summarizes the results of this study and points out the possible implication of the findings on the models of planet obliquities.

2. KOI SAMPLE

For this work we used the list of the KOIs and their parameters from the NASA Exoplanet Archive[4] (NEA; Akeson et al. 2013) of 2014 March 25. Targets identified as false positives by either the *Kepler* pipeline or the NEA were excluded, leaving 3685 KOIs.

Targets listed as EBs on the Villanova Eclipsing Binary web site[5] were removed from the sample. Admittedly, some of the systems in the EB catalog are probably giant, sometimes inflated, planets. Kepler-76 (Faigler et al. 2013) is one example. Nevertheless, we preferred to lose a small number of planets than contaminating our sample with many EBs. The EB website hosts an up-to-date and extended version of the *Kepler* EB catalogs of Prša et al. (2011) and Slawson et al. (2011). The EB catalog used in this work was downloaded on 2014 April 1, and included 302 targets in our KOI sample. Five stars had neither *Kepler* Input Catalog (KIC) or NEA $T_{\rm eff}$ available so were also removed from the sample. We were left with 3355 host stars, which are listed in Table 1.

The effective temperatures and surface gravities used in this work come from the KIC (Brown et al. 2011) or, when available, from Dressing & Charbonneau (2013). Targets with parameters

[4] http://exoplanetarchive.ipac.caltech.edu
[5] http://keplerebs.villanova.edu

from Dressing & Charbonneau (2013) have the "D" flag set in Table 1. For 121 stars in the sample that are missing KIC values for $\log g$ and $T_{\rm eff}$, we used those provided in the NEA. These objects have the "N" flag set in Table 1.

We performed additional binarity checks and identified eight KOIs as likely EBs due to depth differences in alternate transits. These are flagged as "F" in Table 1 and excluded from the study, leaving 3347 targets.

We used the $\log g$ and $T_{\rm eff}$ cut of Ciardi et al. (2011) to identify 138 likely giants, which have the "G' flag set in Table 1. Three of these were previously excluded as likely false positives from this work (flag "F'). The likely giants were excluded from the analysis because we focus on main-sequence stars only.

The temperatures of most stars in our KOI sample were found in the range of 3500–6500 K. Only 124 stars hotter than or equal to 6500 K or cooler than or equal to 3500 K are listed in Table 1. We have opted to exclude them from the analysis, in order to enable us to concentrate on a well defined temperature range that included most of the stars. The rejected KOIs are noted by the "T" flag in Table 1. Two of these were previously excluded as likely false positives (flag "F') and one as a likely giant (flag "G"). This provides a total of 3091 stars to which the automated autocorrelation function (AutoACF) was applied.

3. ROTATIONAL PERIOD MEASUREMENT

McQuillan et al. (2013b) already derived the rotational periods of 737 KOIs. Since then the list of KOIs and EBs were updated and more quarters became publicly available. We therefore performed the search for rotational photometric modulation again, now using the public release 14 quarter 3–14 (Q3–Q14) LCs, which were downloaded from the *Kepler* mission archive.[6] We omitted Q0 and Q1 due to their short duration and Q2 because of significant residual systematics. We used the data corrected for instrumental systematics using PDC-MAP (Smith et al. 2012; Stumpe et al. 2012), which removes the majority of instrumental glitches and systematic trends using a Bayesian approach, while retaining most real (astrophysical) variability. Of the 3685 KOIs, 3662 had publicly available PDC-MAP Q3-Q14 LCs.

The rotational period measurement was performed using the AutoACF technique, described in detail in MMA14. This method is based on the measure of the degree of self-similarity of the LC over a range of lags. In the case of rotational modulation, the repeated spot-crossing signatures lead to ACF peaks at lags corresponding to the rotational period and integer multiples of it. The basic pre-processing steps applied to the PDC-MAP LCs are described in McQuillan et al. (2013a, 2013b), including median normalization of each quarter and masking transit events.

The automation of the detection method uses a training set of visually verified ACF results to select only period detections with high probability of being true rotational measurements, based on the ACF peak height, its period, and the stellar temperature $T_{\rm eff}$, and the consistency of the detection in different sections of the LC. A detailed description is given by MMA14. KOIs with inconsistent detections in different quarters were flagged by M1 in the table, and the ones with peaks not high enough, depending on the temperature and period, by M2. The AutoACF yielded 1031 period detections. Since there are a small number of KOIs compared to the full sample for which the automation routine was developed, we also visually examined all AutoACF periodic KOI detections, and removed 19 targets which either had false period detections, or the period did not appear to arise from rotational modulation. These have the "R" flag set in Table 1.

The visually verified AutoACF analysis yielded 1012 period detections. We found that for 18 of these targets, the centroid motions on the *Kepler* CCD indicate that the transits and rotation are on different targets (flag "C"). A single star, KIC 8043882, was removed from the sample because a valid amplitude of modulation measurement could not be made due to missing data sections.

Once these potential contaminants were removed, we were left with 993 period detections for main-sequence planet hosts, upon which this study focused. As in MMA14, to derive the photometric amplitude we divided the LC of each KOI into time bins of the detected rotational period, obtained the photometric difference between the 5th and the 95th percentiles of normalized flux for all time bins, and then took the median of these values. The detected periods were between 0.2 and 65 days, and the amplitude of the modulation, $R_{\rm var}$, ranges from 0.1 to 100 mmag.

4. COMPARISON WITH *KEPLER* SINGLE STARS

To compare the KOIs with the *Kepler* single-star sample we use the results of MMA14, who reported rotational periods for 34,030 main-sequence stars observed by *Kepler*. The selection criteria for these targets were described in detail in MMA14, and included the same $T_{\rm eff}$ and $\log g$ cuts for main sequence as are used in the present paper, as well as removal of known KOIs and EBs. For the present work we constrain the $T_{\rm eff}$ range to 3500–6500 K, leaving a total sample of 33,614 single stars.

To compare the amplitudes of photometric modulation of the KOIs to those of the single stars of the *Kepler* sample, we plot in Figure 1 the amplitudes of the stars in the two samples as a function of the stellar temperature. In addition, each of the two samples are divided into 250 K temperature bins, and the median of each bin is plotted. The scatter of each bin is estimated by its MAD—the median of the absolute deviation of the amplitudes with respect to the median of each bin, multiplied by 1.48. We prefer the MAD estimate as it is less sensitive to the outliers. The error on the median of each bin, also plotted in the figure, is the MAD$/\sqrt{n}$ of the sample in each bin, where n is the number of points per bin. The figure also displays for each sample a running median, with 1000 and 250 points width for the single and the KOIs amplitudes, which were then smoothed with a width of 501 and 51 points, respectively.

Figure 1 suggests that the KOIs have typically larger amplitudes than the single stars for all but the hottest two $T_{\rm eff}$ bins, 6000–6500 K, which show significantly lower amplitudes for the KOIs. To check the significance of the differences, we show in Figure 2 the results of a two-sample Kolmogorov–Smirnov (K-S) test for the KOIs and the single stars, performed for separate two temperature ranges—3500–6000 and 6000–6500 K. The p values for the null hypothesis, which assumes that the KOIs and the single stars are both drown from the same underlying amplitude distribution, are shown above the two panels of Figure 2. The p values of the two-sample K-S test, 3.2×10^{-6} and 9.1×10^{-6}, for the two temperature bins, respectively, suggest that the differences between the KOIs and the single stars are highly significant in both ranges of temperatures.

5. SELECTION EFFECTS?

The amplitude distributions of the KOIs and the single stars seem significantly different. However, before we can conclude

[6] http://archive.stsci.edu/kepler

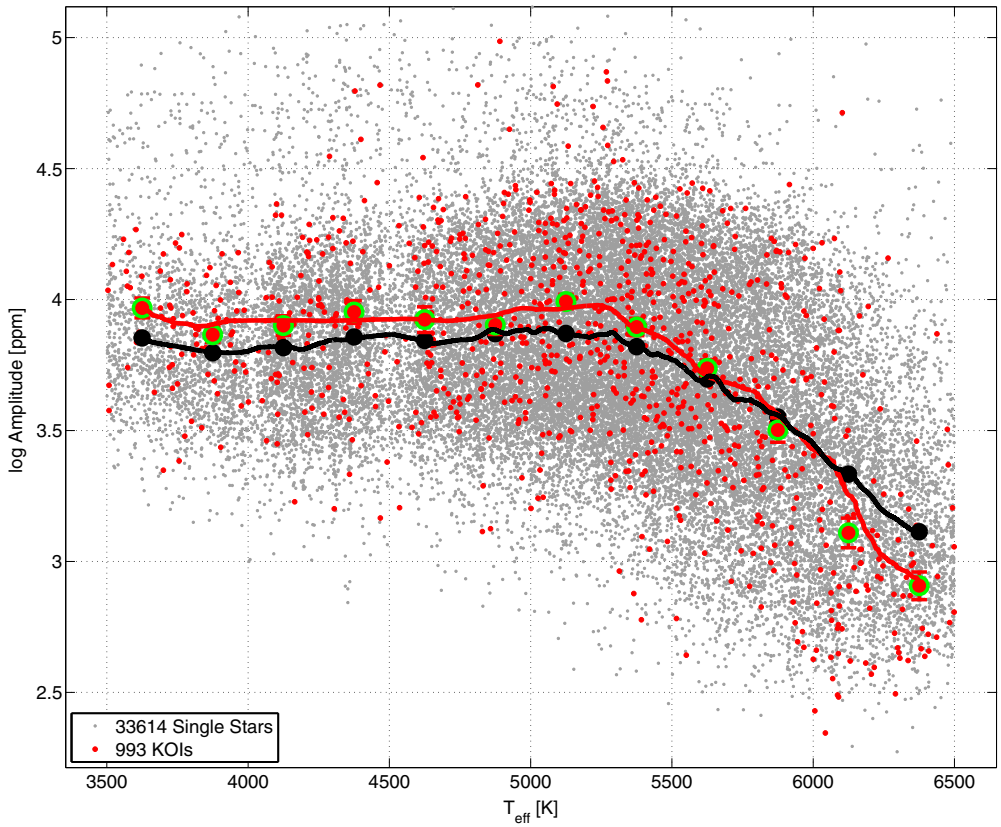

Figure 1. Derived amplitudes of the photometric stellar rotation for *Kepler* single stars and KOIs as a function of stellar temperature. There are 33,614 (black) single stars and 993 (red) KOIs in the figure. Amplitudes are given by their log values in ppm. Each of the two samples are divided into 250 K temperature bins, and the median of each bin is plotted. The error on the median is the MAD/$\sqrt{n}$ of the sample in each bin, where n is the number of points per bin. For most bins, the error bars are smaller than the points. Also plotted are the running medians of each sample (see the text).

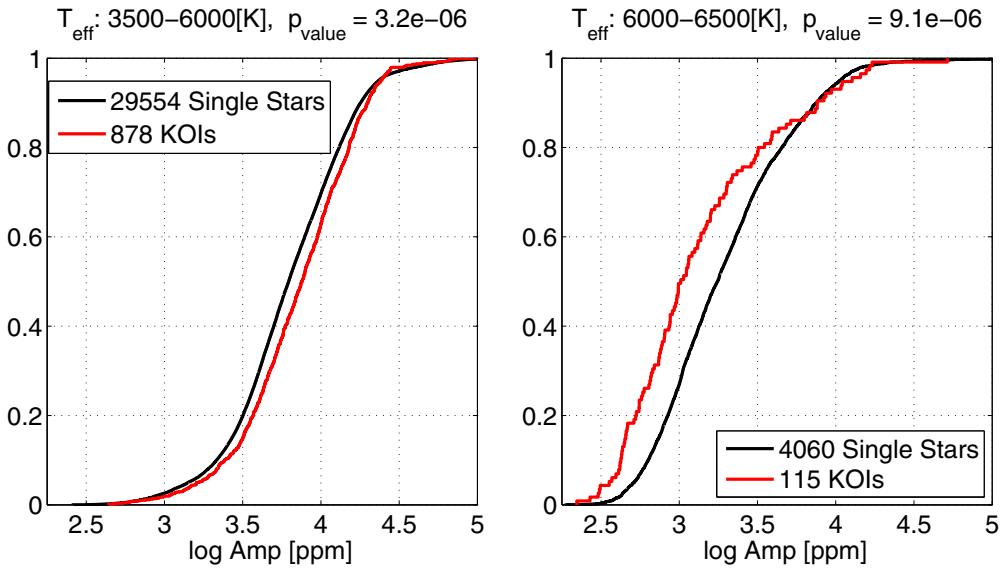

Figure 2. Cumulative distributions of the photometric amplitudes of the *Kepler* single stars and the KOIs for two ranges of stellar temperatures. The left panel shows the distributions of the amplitudes of the cool stars, at a range of 3500–6000 K. Red is for the KOIs and black for the single stars. The right panel shows the distributions for the hot stars, 6000–6500 K. The p value of the two-sample K-S test for each range of temperatures is also given.

that this is indirect evidence for a small star–planet obliquity of the cool stars and a high obliquity of the hot stars we have to consider possible selection effects that could have caused the amplitude differences. We consider in this section two possible such observational biases, one that has to do with the rotational periods of the KOIs and the single stars, and the other with stellar noise of the hot stars that determines the transit detection threshold.

To consider the period issue, we constructed in each temperature bin a series of single-star subsamples with rotational period distributions similar to that of the KOIs, and showed that we obtain the same amplitude difference as with the real single-star

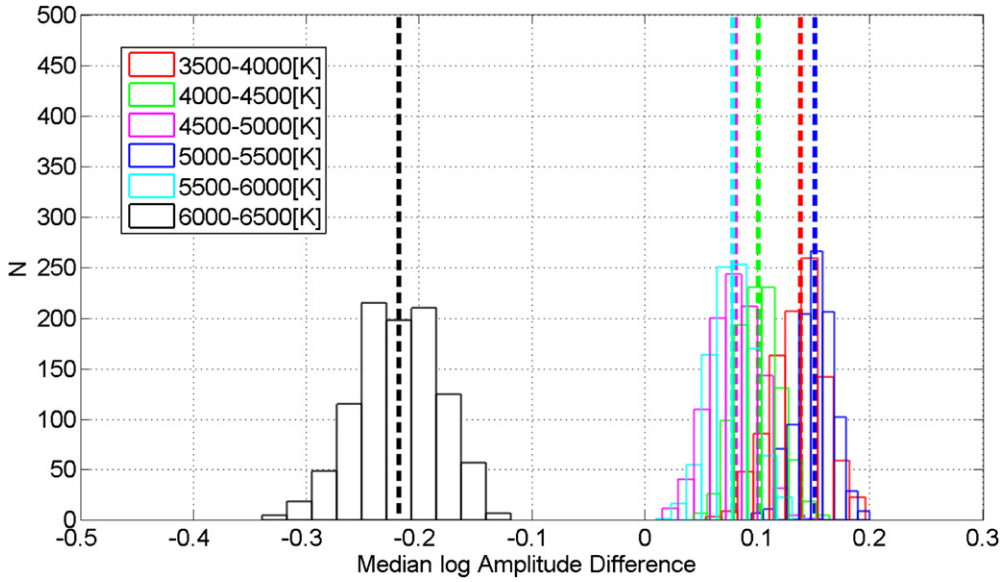

Figure 3. Differences between the median log-amplitudes of the KOIs and the single stars *with the same period distribution* for several temperature bins. Histograms show the differences of the log-amplitude medians derived for 1000 random (see the text) single-star subsamples. The median of the differences for each $T_{\rm eff}$ bin is shown by a vertical dashed line. The colors present the different temperature bins.

sample. To study the problem of the stellar noise and the detection threshold, we generated a series of randomly simulated hot KOI samples that could have been detected, and compare their amplitudes with those of the real KOI and single-star samples. We find that the detection bias introduces a decrease in the KOI's amplitudes, but the actual sample of KOIs displays a difference too large to be accounted for by the selection effect and is probably due to high obliquity.

5.1. Rotational Periods

Rotational periods and amplitudes are known to be correlated (e.g., Pizzolato et al. 2003; Hartman et al. 2011; MMA14), with typically higher amplitude variability at shorter periods. Therefore, the amplitude difference we observe could be a result of a difference between the rotational periods of the KOIs and those of the single stars. To face this problem, we performed a follow-up test of comparison, with matching period distributions for the KOI and the single-star samples, to remove any possible bias introduced by different period distributions. We divided the sample into bins of 500 K, selecting for each $T_{\rm eff}$-bin a *random* sample of single stars that approximately matched the period distributions of the KOIs of that temperature, and compared the median amplitudes of the KOIs and the single stars in each bin.

This was done by dividing the period distributions into 10 bins of width 0.25 in log period between -0.5 and 2, in days, with two additional bins for periods outside this range. We then selected a random sample of single stars, with twice the number of stars in each period bin as were in the KOIs sample for the same period bin. This was the maximum integer multiple possible in all $T_{\rm eff}$ and period bins. We then derived for each random choice of the single-star sample its median value. This process was then repeated 1000 times, with a new random sample of non-KOIs drawn each time, and the same full sample of KOIs used in each run. For each random sample we derived the difference between the median of the log amplitudes of the KOIs and the single stars, obtaining for each temperature bin a distribution of differences of medians, which were plotted in Figure 3.

Figure 3 is consistent with the picture revealed by the two previous ones. For the cool stars, the KOIs have, on the average, larger amplitudes than the single ones, on the order of 0.1 in log amplitude, or a factor of $\simeq$1.25 larger. The hot KOIs, on the other hand, have smaller amplitudes, on the order of 0.2 in log amplitude or a factor of $\simeq$0.6 smaller.

We therefore conclude that the amplitude difference we observe is *not* a result of a period difference between the KOIs and the single stars.

5.2. Stellar Noises and the Hot Stars

As pointed out by the anonymous referee, the small amplitudes of the hot stars could have been the result of observational selection effect. In his/her wise words, "planets are more challenging to detect around stars with high variability, causing their stellar variability to appear systematically lower. This could be an issue for the hot stars which, on the main sequence, are larger than cool stars, making it more difficult to detect... planets except around the least variable stars."

In order to estimate the magnitude of the contribution of the selection effect induced by the planet detection, following the referee's suggestion, we have generated 100,000 *simulated* samples of "planets around hot stars," for which their parent stars where randomly chosen under *Kepler* discovery constraints. The goal is to find out how many of the simulated samples showed small amplitudes like the real sample, in order to estimate the significance of the amplitude difference between the KOIs and the hot single stars.

To form a simulated sample associated with the observed planets we have considered two real samples—the sample of planets orbiting hot stars with detected rotational periods (115 systems; Sample $\mathcal{P}$) and the sample of all hot stars with known rotational periods and amplitudes, including the KOIs with known periods (4147 systems; Sample $\mathcal{R}$). For each planet $\{P_i \in \mathcal{P}, i = 1:115\}$, we constructed a subsample, $\mathcal{R}_i$, chosen from the large sample $\mathcal{R}$, consisting of stars that could have been the parent star of P_i and still be detected, given the stellar radius and photometric noise. A simulated sample of KOIs was then constructed by choosing randomly a star from each of the subsamples $\{\mathcal{R}_i, i = 1:115\}$.

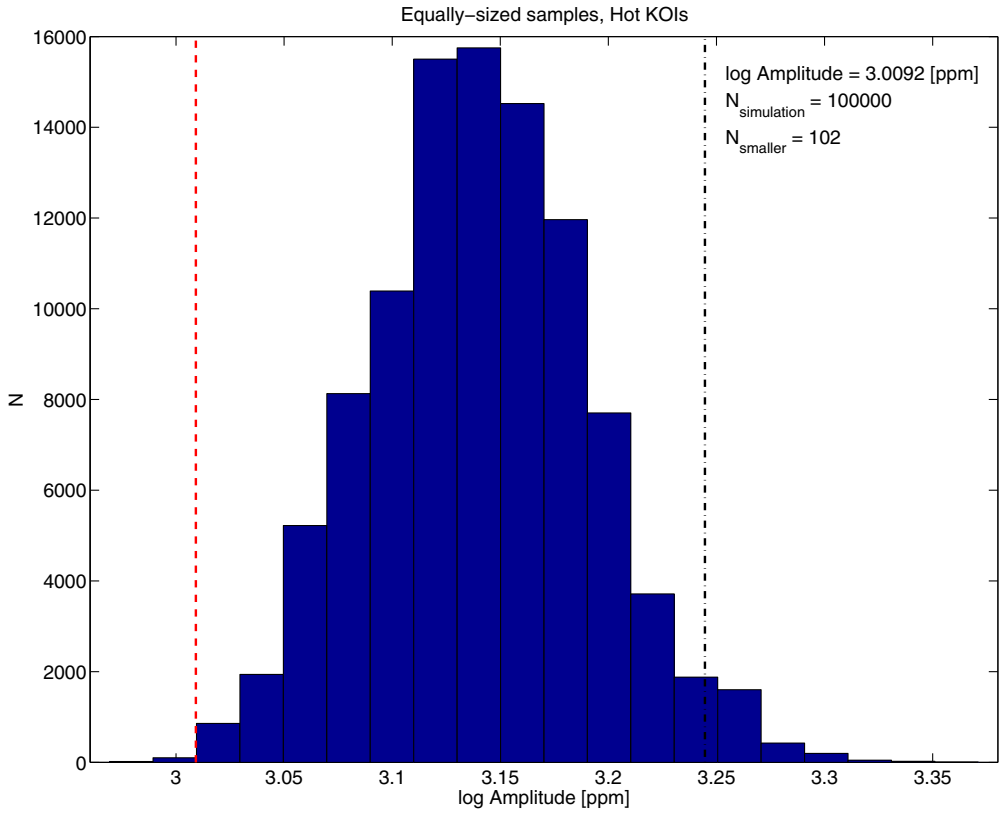

Figure 4. Histogram of the median values of the amplitudes of 100,000 simulated samples of 115 planets around hot stars (see the text). Also marked are the value of the real sample (in dashed red line) and median of all the hot stars (in dashed-dot blue line).

For a star to be considered as a potential parent star to a planet P_i and therefore included in the $\mathcal{R}_i$ simulated sample, we required the potential star to have signal-to-noise ratio S/N $\geqslant$ 10, had it had the P_i around it, in the case of the actual transit $\{S/N\}_i \geqslant 10$, and S/N $\geqslant \{S/N\}_i$, if the actual transit $\{S/N\}_i < 10$.

To derive the potential S/N, we used the Howard et al. (2012) expression, which we write here as

$$S/N = \frac{R_{pl}^2}{\sigma_{CDPP} R_*^2} \sqrt{\frac{n_{tr} \cdot t_{dur}}{3\ \mathrm{hr}}}, \quad (1)$$

where n_{tr} is the number of observed transits, t_{dur} is the transit duration, R_* and R_{pl} are the stellar and planet radii and σ_{CDPP} is the 3 hr photometric noise of *Kepler*. In fact, the *Kepler* site includes such a noise estimate for each observed quarter, so we used the median of these values, $\bar{\sigma}_{CDPP}$, for our simulations. The stellar radius was estimated from the stellar mass, M_*, derived by McQuillan et al. (2014), assuming a main-sequence $R_* \propto M_*^{0.8}$ relation. We also assume that $t_{dur} \propto R_*$, and therefore conclude that for a given planet,

$$S/N \propto \frac{1}{\bar{\sigma}_{CDPP} R_*^{3/2}}\ . \quad (2)$$

We performed 100,000 simulations, each of which produced a simulated sample of hot stars with detected rotational periods and amplitudes, with enough S/N so the planets could have been detected. To compare the simulated sample with the real one we used two metrics—the median of the amplitudes and the p value of the two-sample K-S test when compared with the whole sample of hot stars. Histograms of the 100,000 derived two measures are plotted in Figures 4 and 5.

The histogram of Figure 4, centered around log-amplitude of ∼3.15 (in ppm units), as opposed to the median of the hot stars at ∼3.25, corroborates the suspicion of the referee—the detection threshold of planets indeed results in smaller amplitudes. The difference in log-amplitude indicates that this effect reduces the amplitudes by a factor of ∼0.8. However, the figure further shows that the median of the real sample of hot KOIs is smaller by another factor of 0.8. This might suggest that the smallness of the amplitudes of the hot KOIs could be due *also* to some geometrical distribution.

How significant is this finding? The simulations presented in the two figures show that out of the 100,000 simulations, only 594 showed a p value of the K-S test smaller than the real one, and only 102 had a smaller median. The implication is that the chance of observing such a difference by a statistical fluke is 0.6%, according to the p value of the K-S test, or 0.1%, if we adopt the median metric. Figure 5 shows that the distribution of the K-S p values has a long tail toward small values, if plotted on the log scale, and therefore might not be the best metric to distinguish between real and fluke result. We tend to adopt the 0.1% result, and contend that the smallness of the hot KOI amplitudes, by a factor of 0.8, is detected with a high statistical significance.

6. THE GEOMETRY OF THE SPIN–ORBIT INCLINATIONS OF THE KOIs

The analysis presented here might have some implication on the geometrical distribution of the spin–orbit inclinations of the KOIs.

Suppose that the observed amplitude of the photometric spot modulation of a given star is proportional to $\sin i_{rot}$, where i_{rot} is

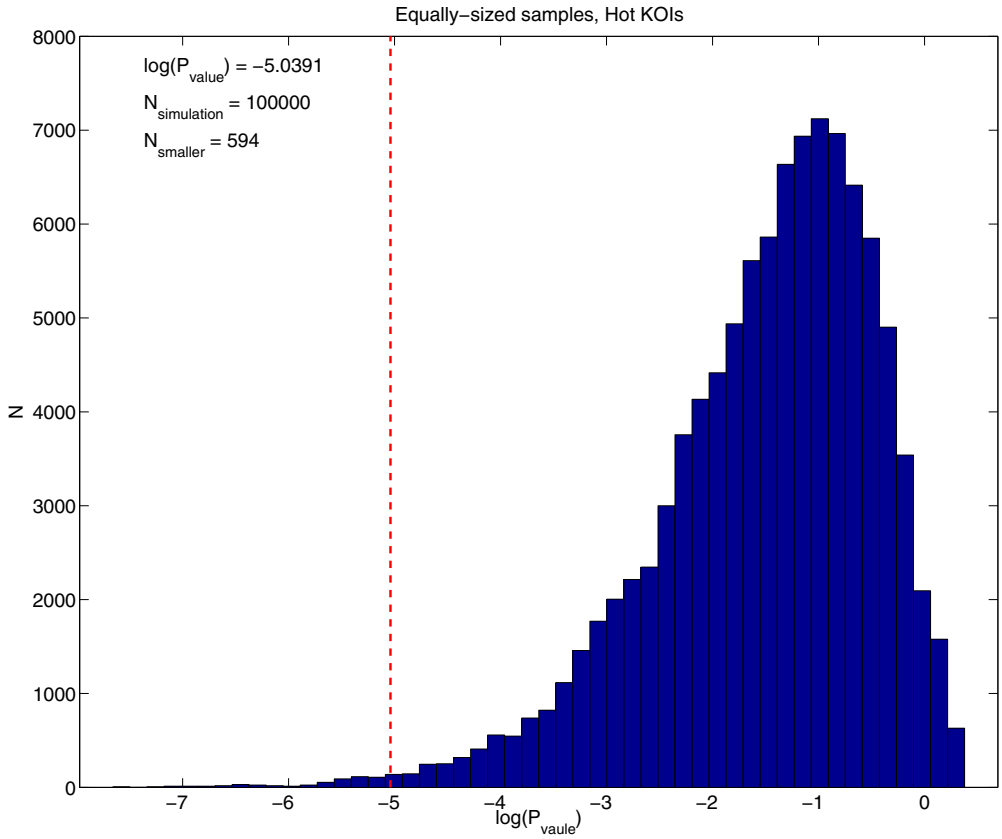

Figure 5. Histogram of the p values of the K-S test, when 100,000 simulated samples of planets around hot stars are compared with the amplitudes of the whole sample of hot stars with detected rotations. Also plotted is the value of the real sample (in dashed red line).

the inclination of the axis of rotation of that star relative to our line of sight (e.g., Jackson & Jeffries 2012). In such a case, we might naively expect that the average amplitude of a *sample* of observed stars should be proportional to the expected value of $\sin i_{\rm rot}$ of the sample—$\langle \sin i_{\rm rot} \rangle$ (Jackson & Jeffries 2013). In real cases we have to consider the convolution of the distribution of the amplitudes with the distribution of inclinations and take into account the detection threshold of the analysis, two factors that complicate the discussion. However, we assume these factors do not change the general picture we are trying to draw here.

Now consider two samples, one with random orientations of its stellar rotational axes in space, with $\langle \sin i_{\rm rot} \rangle = \pi/4$, and the other sample with all stars having $i_{\rm rot} \simeq 90^\circ$, all other features being equal. We then expect the ratio of the two amplitude averages of the two samples to be of the order of $4/\pi \simeq 1.25$.

This is indeed close to what we get for the cool stars, when we compare the rotational amplitudes of the KOIs and those of the single stars of the *Kepler* mission. We do find that the median of the amplitudes of the cool KOIs is larger by a factor of $\simeq$1.25 than the median of the single star amplitudes. If we assume that the spin axes of the single stars are randomly oriented, then our analysis suggests that the stellar spin of the KOIs have their rotational inclination close to 90°. This is consistent with the assumption that the spin axes of the cool KOIs are aligned with the angular momentum of their transiting planets, which must have their *orbital* inclination close to 90°.

An opposite picture is revealed for the hot KOIs. The median amplitude of the hot KOIs is probably *smaller* by the same factor, $\sim$1.25, when compared to the median of the amplitudes of the single stars, taking into account the detection bias. This also might be accounted for by a geometrical effect. The maximum geometrical suppression of $\langle \sin i_{\rm rot} \rangle$ due to spin–orbit misalignment is achieved when all rotational axes are orthogonal to the orbital axes, which have their orbital inclinations close to 90°. This leads to $\langle \sin i_{\rm rot} \rangle = 2/\pi$, while for random orientation $\langle \sin i_{\rm rot} \rangle = \pi/4$. Therefore, the reduction factor of $\langle \sin i_{\rm rot} \rangle$ is about $1/1.25$. Obviously, any other geometrical spin–orbit distribution (e.g., Morton & Winn 2014) should result in a less dramatic reduction. Again, the convolution with the distribution of the amplitudes and the detection bias are going to blur the picture even more. Nevertheless, the fact that the simplest approach yields a factor similar to the one inferred from the analysis is encouraging.

We wish to call attention to two caveats of the analysis presented here.

1. Our analysis is not sensitive to the difference between prograde and retrograde rotational inclinations, as the amplitude depends on the absolute value of $\sin i_{\rm rot}$. Namely, the cool KOIs, for which our analysis suggests rotational axes aligned with the planetary orbital motion, could have prograde or retrograde motion. Different approaches, like the one suggested by Mazeh et al. (2014), can shed some light, admittedly for only a very small number of cases, on this question.
2. We tried to look for differences between large and small planets, but could not convince ourselves, after the referee's doubts in particular, that the results are real, and not due to some observational biases. We suspect that the indirect approach of the present work is not capable of distinguishing between the large and small planets.

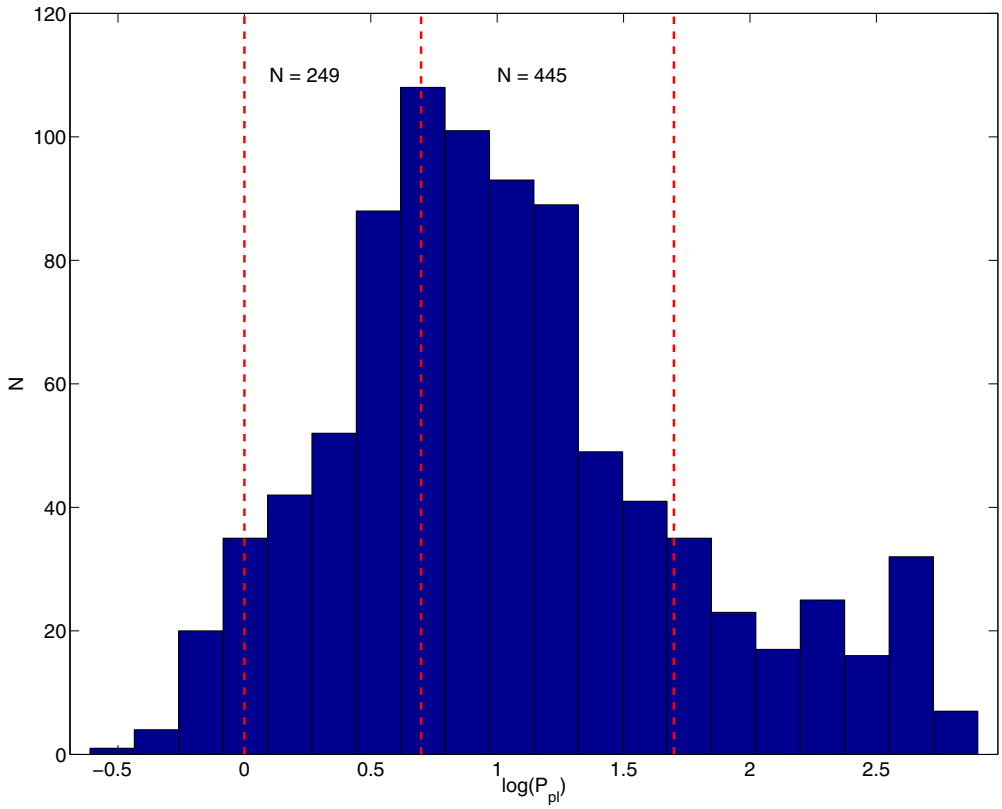

Figure 6. Histogram of the orbital periods of the innermost planets of the cool KOIs with detected photometric rotation. The three dashed lines show the two period ranges compared here.

7. SHORT AND LONG ORBITAL PERIODS AROUND COOL KOIs

After showing that the larger photometric amplitudes of the cool KOIs might be an indication for low obliquity of their planets, it is of interest to find out if this phenomenon is limited only to KOIs with short orbital periods, or it extends to the long periods. We therefore divided the cool KOIs into two period ranges, somewhat arbitrarily, of *innermost* orbital periods of 1–5 days and 5–50 days, as indicated in the orbital-period histogram, plotted in Figure 6. Planets with orbital periods outside the range 1–50 days might be too close or too far away from their parent stars to show the general trend we wish to study.

In Figure 7 we plot the cumulative distributions of the photometric amplitudes of the cool KOIs with short (1–5 days) and long (5–50 days) orbital periods. Distributions of all cool KOIs and *Kepler* single stars are given for reference. The medians and the p value of the two-sample K-S test for the different samples are given too. The figure shows that the two subsamples have very similar amplitudes, with almost identical medians, distinctively different from the single cool stars. This suggests that the feature we have discovered—the larger photometric rotational amplitudes of the cool KOIs, is not only restricted to short orbital periods, but extend up to periods of 50 days. In our suggested interpretation, the low obliquity of planets around cool stars extends up to at least 50 days.

8. SUMMARY AND DISCUSSION

In this study we compare the amplitude distribution of the rotation of 993 KOIs with the amplitudes of 33,614 single stars observed by the *Kepler* mission in temperature range of 3500–6500 K, in order to shed some light on the statistical distribution of spin–orbit obliquity of the planetary systems.

The analysis presented here is rather limited because (1) the observed distribution of the amplitudes of any KOI sample is the result of the convolution of the true obliquity with the real amplitude distribution of the sample, (2) we are sensitive only to the line of sight inclination and not to the true obliquity, and (3) our measurements are subject to observational biases. The latter is stronger for smaller planets and hot stars. Although we can try and debias the observations, this inserts a high degree of uncertainty into our results. On the other hand, the analysis presented here does not require any additional observational resources and can be applied to a large sample of KOIs, with short and long orbital periods alike.

The comparison between the amplitude distributions shows that in the temperature range of 3500–6000 K the amplitudes of the KOIs are larger, on the order of 10%, than those of the single stars, consistent with the assumption that the spin–orbit obliquity is rather small for cool stars. The low obliquity extends up to at least 50 days. For the hot stars, with a temperature range of 6000–6500 K, we have found the opposite effect. The amplitudes of the hot KOIs are probably *smaller* by the same factor, of the order of 10%, when compared to the amplitudes of the single stars, taking into account the detection bias. This could be the result of the high obliquity of the hot stars. Our findings are consistent with Winn et al. (2010) and Albrecht et al. (2012), who discovered such a transition between aligned and non-aligned systems at about 6250 K.

The analysis presented here might shed some light on the mechanism responsible for the spin–orbit dichotomy between planets around cool and hot stars. In their seminal paper, Winn et al. (2010) discussed two possible scenarios to account for

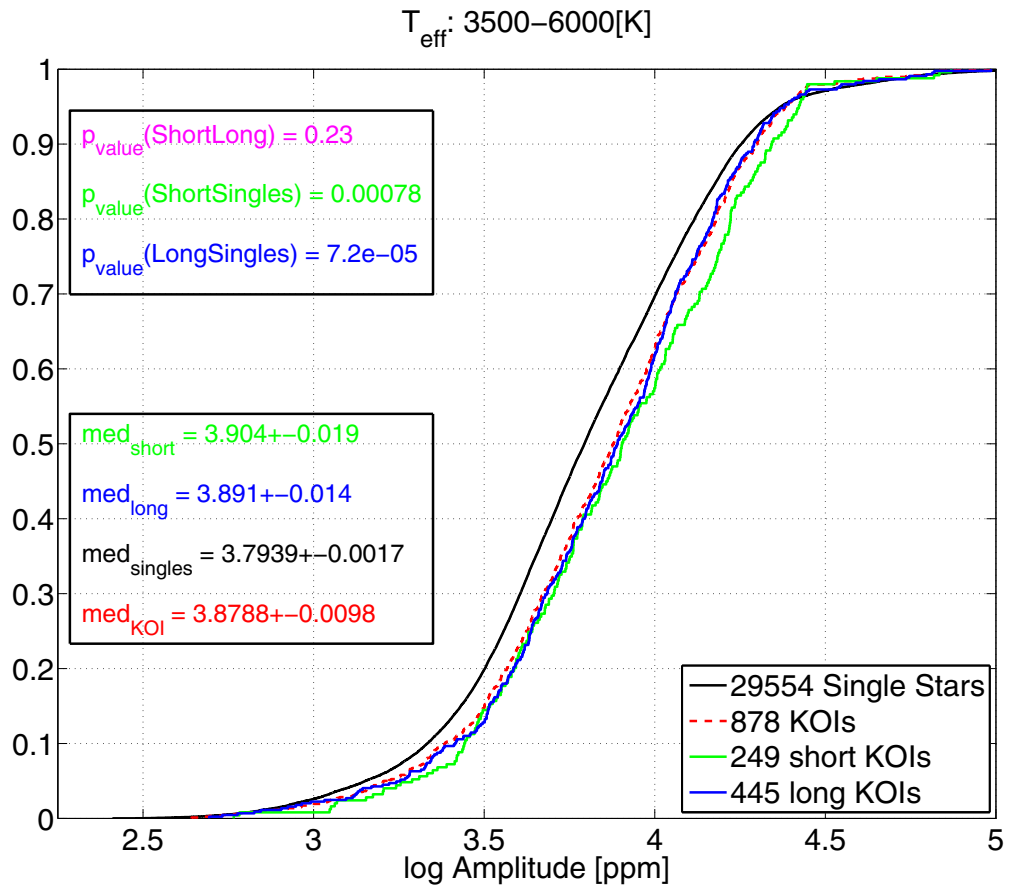

Figure 7. Cumulative distributions of the photometric amplitudes of the cool KOIs with short (1–5 days) and long (5–50 days) orbital periods. Distributions of all cool KOIs and *Kepler* single stars (Figure 2, left panel) are given for reference. The medians and the *p* value of the two-sample K-S test for the different samples are given as well.

their findings. The first had to do with formation mechanism—planets around hot stars might have originally formed with high obliquities, while planets around low-mass stars have been formed with low obliquities (see also Lai 2014; Batygin 2012). Winn et al. (2010) then focused on a different scenario, where the spin–orbit dichotomy arises from a later evolution of the system. In their scenario planets go through a high obliquity phase, probably due to planet–planet scattering, which is then followed by a long tidal interaction period. The tidal interaction affects hot and cool stars differentially. Winn et al. (2010) suggested that since cool stars have convective envelopes, their tidal interaction with the planets is more effective, leading to the alignment of the planetary orbit with the rotation of its host cool star. Conversely, hot stars, whose envelopes are radiative, cannot align the planetary orbits.

Within the tidal realignment models, the alignment timescale depends on the planet's separation from its host star. Such models therefore predict that only short-period planets should be aligned with their host star's rotation, as the tidal realignment becomes negligible for long-period planets. Our results are probably not aligned with this prediction, because we find evidence that the small obliquity of the cool KOIs extends to at least 50 days, while the tidal planet–star interaction is probably not very effective in long, 10–50 days, orbital periods.

Kepler provided us with the rare capability of studying a sample of about 150,000 almost uninterrupted LCs, out of which we discovered thousands of new planets and tens of thousands stellar rotations. The combination of the two can be used as a new tool to explore the characteristic statistical features of planet–star interaction, of which this study is an example. To better exploit this exciting opportunity, investigating the planet–star obliquity in particular, we should combine different techniques, like RM effect, the line-broadening approach, asteroseismology, and spot crossing analysis, applied to specific systems, together with statistical approaches like the one presented here. This could reveal more features of the obliquity and its dependence on stellar temperature and planetary mass and orbital period, and shed some light on the formation and evolution of planetary systems.

We are indebted to the referee for very thoughtful advice that substantially improved the previous version of the paper. We wish to deeply thank Tomer Holczer for his tests to identify EB contamination, Gil Nachmani, Suzanne Aigrain and Simchon Faigler for illuminating and helpful discussions, and Eric Agol for useful comments. The research leading to these results has received funding to T.M. from the European Research Council under the EU's Seventh Framework Programme (FP7/(2007-2013)/ERC grant agreement No. 291352). T.M. also acknowledges support from the Israel Science Foundation (grant No. 1423/11). T.M. and H.B.P. acknowledge support from the Israeli Centers of Research Excellence (I-CORE, grant No. 1829/12). H.B.P. acknowledges support from the European Union's—Seventh Framework Programme (FP7/2007-2013]) under grant agreement No. 333644–MC–GRAND, as well as the "Minerva center for life under extreme planetary conditions." T.M. is grateful to the Jesus Serra Foundation that enabled an extended visit to the Instituto de Astrofísica de Canarias, and to

his hosts, Hans Deeg and Rafael Rebolo in particular. The last phase of this work has been completed during this visit. This research has made use of the NASA Exoplanet Archive, which is operated by the California Institute of Technology, under contract with the National Aeronautics and Space Administration under the Exoplanet Exploration Program. All of the data presented in this paper were obtained from the Mikulski Archive for Space Telescopes (MAST). STScI is operated by the Association of Universities for Research in Astronomy, Inc., under NASA contract NAS5-26555. Support for MAST for non-*HST* data is provided by the NASA Office of Space Science via grant NNX09AF08G and by other grants and contracts.

REFERENCES

Akeson, R. L., Chen, X., Ciardi, D., et al. 2013, PASP, 125, 989
Albrecht, S., Winn, J. N., Johnson, J. A., et al. 2012, ApJ, 757, 18
Basri, G., Walkowicz, L. M., Batalha, N., et al. 2011, AJ, 141, 20
Batalha, N. M., Rowe, J. F., Bryson, S. T., et al. 2013, ApJS, 204, 24
Batygin, K. 2012, Natur, 491, 418
Borucki, W. J., Koch, D., Basri, G., et al. 2010, Sci, 327, 977
Brown, T. M., Latham, D. W., Everett, M. E., & Esquerdo, G. A. 2011, AJ, 142, 112
Chaplin, W. J., Sanchis-Ojeda, R., Campante, T. L., et al. 2013, ApJ, 766, 101
Ciardi, D. R., von Braun, K., Bryden, G., et al. 2011, AJ, 141, 108
Dawson, R. I. 2014, ApJL, 790, L31
Dressing, C. D., & Charbonneau, D. 2013, ApJ, 767, 95
Fabrycky, D. C., & Winn, J. N. 2009, ApJ, 696, 1230
Faigler, S., Tal-Or, L., Mazeh, T., Latham, D. W., & Buchhave, L. A. 2013, ApJ, 771, 26
Gizon, L., & Solanki, S. K. 2003, ApJ, 589, 1009
Hartman, J. D., Bakos, G. A., Noyes, R. W., et al. 2011, ApJ, 141, 166
Hébrard, G., Ehrenreich, D., Bouchy, F., et al. 2011, A&A, 527, L11
Hirano, T., Sanchis-Ojeda, R., Takeda, Y., et al. 2012, ApJ, 756, 66
Hirano, T., Sanchis-Ojeda, R., Takeda, Y., et al. 2014, ApJ, 783, 9
Howard, A. W., Marcy, G. W., Bryson, S. T., et al. 2012, ApJS, 201, 15
Jackson, R. J., & Jeffries, R. D. 2012, MNRAS, 423, 2966
Jackson, R. J., & Jeffries, R. D. 2013, MNRAS, 431, 1883
Lai, D. 2014, MNRAS, 440, 3532
Mazeh, T., Holczer, T., & Shporer, A. 2014, ApJ, in press (arXiv:1407.1979)
McQuillan, A., Aigrain, S., & Mazeh, T. 2013a, MNRAS, 432, 1203
McQuillan, A., Mazeh, T., & Aigrain, S. 2013b, ApJL, 775, L11
McQuillan, A., Mazeh, T., & Aigrain, S. 2014, ApJS, 211, 24
Morton, T. D., & Winn, J. N. 2014, ApJ, 796, 47
Moutou, C., Díaz, R. F., Udry, S., et al. 2011, A&A, 533, A113
Nielsen, M. B., Gizon, L., Schunker, H., & Karoff, C. 2013, A&A, 557, L10
Nutzman, P. A., Fabrycky, D. C., & Fortney, J. J. 2011, ApJL, 740, L10
Pizzolato, N., Maggio, A., Micela, G., Sciortino, S., & Ventura, P. 2003, A&A, 397, 147
Prša, A., Batalha, N., Slawson, R. W., et al. 2011, AJ, 141, 83
Queloz, D., Eggenberger, A., Mayor, M., et al. 2000, A&A, 359, L13
Reinhold, T., Reiners, A., & Basri, G. 2013, A&A, 560, A4
Sanchis-Ojeda, R., Winn, J. N., Holman, M. J., et al. 2011, ApJ, 733, 127
Sanchis-Ojeda, R., Winn, J. N., Marcy, G. W., et al. 2013, ApJ, 775, 54
Schlaufman, K. C. 2010, ApJ, 719, 602
Slawson, R. W., Prša, A., Welsh, W. F., et al. 2011, AJ, 142, 160
Smith, J. C., Stumpe, M. C., Van Cleve, J. E., et al. 2012, PASP, 124, 1000
Stumpe, M. C., Smith, J. C., Van Cleve, J. E., et al. 2012, PASP, 124, 985
Triaud, A. H. M. J., Collier Cameron, A., Queloz, D., et al. 2010, A&A, 524, A25
Walkowicz, L. M., & Basri, G. S. 2013, MNRAS, 436, 1883
Winn, J. N., Fabrycky, D., Albrecht, S., & Johnson, J. A. 2010, ApJL, 718, L145
Winn, J. N., Howard, A. W., Johnson, J. A., et al. 2011, AJ, 141, 63